Electronic Supplementary Material (ESI) for Green Chemistry.
This journal is © The Royal Society of Chemistry 2021

Supporting Information

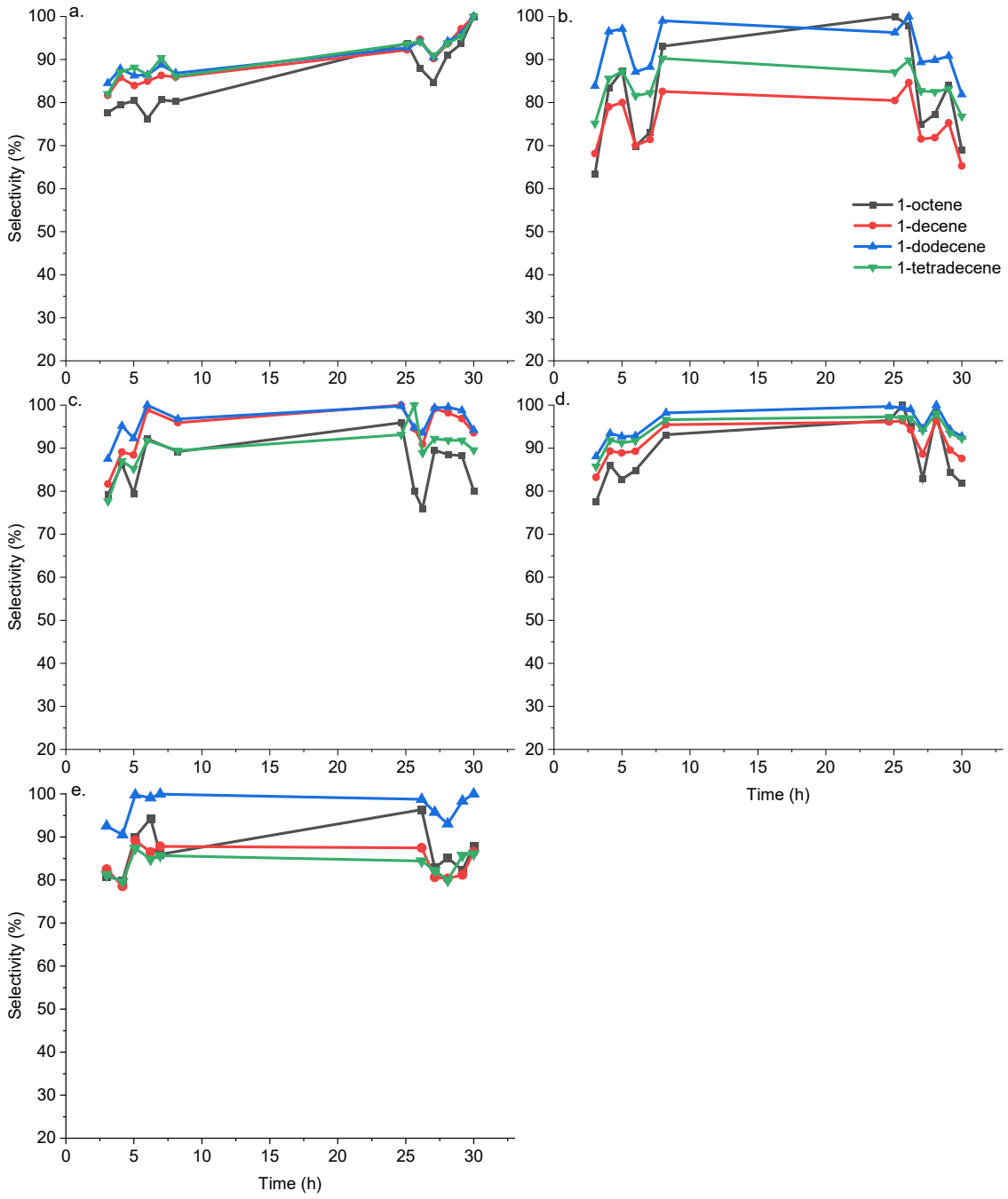

Figure S1. Selectivity of a. simulated primary alcohol feed, b. biologically derived alcohol feed, c. simulated primary alcohol feed doped with C_8 and C_{10} acetate impurities, d. simulated primary alcohol feed doped with extracted LB broth components, and e. simulated primary alcohol feed doped with fatty acids. Reaction conditions: 0.02 mL/min feed flowrate, 350ºC reactor temperature, 50 mL/min He purge gas flowrate, 50 mg 15%Cs/SiO_2 catalyst, and 65 psia backpressure.

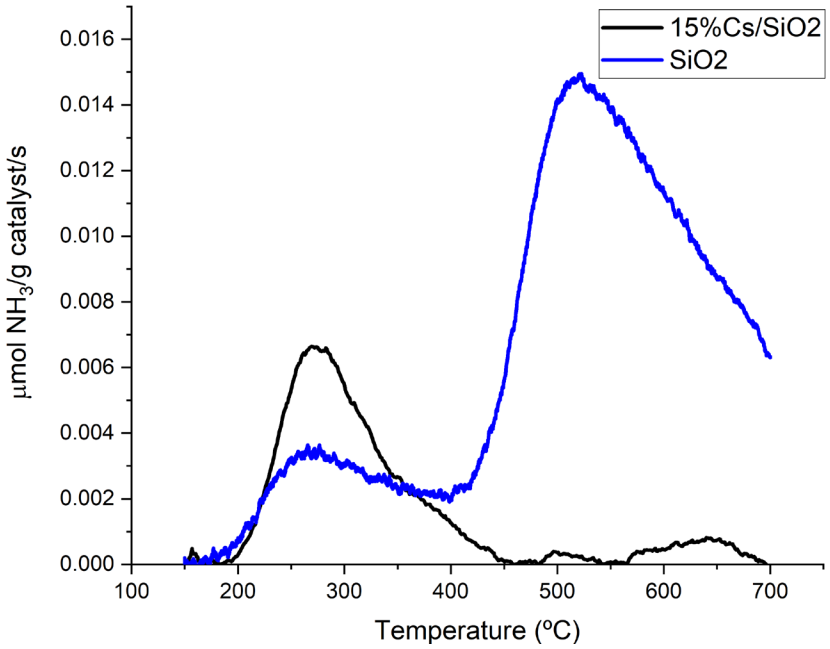

Figure S2. NH_3 TPD of 15% Cs/SiO_2 and SiO_2 highlighting acid site quantity and strength.

Fatty Alcohol Production by Fermentation

In the fermentation section, the glucose is fermented by yeast to produce fatty alcohols including hexanol, octanol, and decanol as described in the following stoichiometric reaction:

Glucose → 1.5 Hexanol + 1.5 Octanol + 4.5 Decanol + H_2O + CO_2 (Equation S1)

The process assumes that the fermentation is selective for lighter fatty alcohols (C6-C10) to simplify the downstream separation scheme. Tridecane is used as an oxygen vector and a solvent for the fermentation products in the fermentation broth. If longer chain fatty alcohols would be produced in the fermenter, additional distillation columns would be required to separate the heavier LAOs from the tridecane solvent, increasing utility costs and capital investment. An alternative process configuration implementing liquid-liquid extraction may be more suitable to separate out a wider range of fatty alcohol chain lengths from the tridecane solvent at an early stage before dehydration.

The fermenter mass balanced is modeled by specifying the fraction of theoretical yield Equation S1 and any remaining glucose is consumed for cell growth. Cell growth in the fermenter is accompanied by the formation of carbon dioxide by assuming that 2 carbons from glucose are used to produce carbon dioxide while the rest of the glucose is used to produce cell mass:

Glucose → 3.72 Cells + 2 CO_2 (Equation S2)

Corn steep liquor (CSL) and diammonium phosphate (DAP) are fed as an economic source of nitrogen and phosphate for cell growth.[1] Low grade salt is also used as a nutrient. The number of reactors are chosen such that the volume of each reactor does not surpass 1 MMGal (3,785 m^3) unless the number of reactors would be greater than 32. Details on the concentration of all chemicals in the fermenter broth are described in Table S1.

Table S1. **Fermentation bioreactor specifications.**

	Baseline Fermentation Performance	**Target Fermentation Performance**
Temperature [°C]	32	32
Reaction time [hr]	45	80
Cleaning and unloading time [hr]	3	3
Loading time [hr]	1.55	6.92
Number of reactors	32	13
Reactor volume [m3]	7,120	3,580
Tridecane in slurry [wt. %]	11.7	11.7
Corn steep liquor (CSL) in slurry [wt. %]	0.25	0.25
Diammonium phosphate (DAP) level in slurry [g·L-1]	0.33	0.33
Dry cell weight level in slurry	0.30 wt %	0.30 wt %
Salt level in slurry	0.585 wt %	0.585 wt %
Yield [% theoretical]	50	80
Titer [g·L-1]	3.5	40
Productivity [g·L-1·hr-1]	0.1	0.5

Unit Operation Modeling, Design, and Purchase Cost

All essential unit operations (i.e. pumps, tanks, heat exchangers, and distillation columns) are designed and costed using BioSTEAM's native unit operations,[1-3] while unit operations specific to this production process (i.e. the fermenters, and adiabatic fixed-bed dehydration reactor) were developed in this study and are only available through the Biodindustrial-Park repository.[4] Descriptions for unit operation modeling and design algorithms, and the size factors used for capital cost estimation in this study, are all detailed in Tables S2 and S3. Modeling refers to the methods used to calculate mass and energy balances while that design refers to the methods used to calculate the size factors for capital cost estimation. Although not shown in the table, the construction material for all pumps, heat exchangers, centrifuges, and vessels (i.e., mixing and storage tanks, flash vessels, and distillation columns) in the biorefinery is stainless steel (SS304). Centrifuge unit operation model separations assuming a certain fraction of chemical components split between output streams. The values of the component splits were back calculated from BioSTEAM's LLE algorithm, which minimizes the Gibb's free energy of the liquid phases by differential evolution. A few unit operations do not have a modeling algorithm as the exit stream is simply equal to the input stream (e.g. tanks and conveyor belts). Unit operations with capital cost size factors based on flow rate do not have a design algorithm as no design is needed to calculate flow rate. Although all heat transfer calculations assume adiabatic conditions, BioSTEAM also presents the option of using a heat transfer efficiency to allow only a fraction of heat to be transferred to the unit operation while the rest is lost to the environment. Considering that high pressure steam is used throughout the biorefineries and heat will be lost in major unit operations such as distillation columns and evaporators, a conservative heat transfer efficiency of 95% was used for steam utilities. Oliveira, Marques and Parise assumed heat losses in an ethanol-water distillation column to be as high as 10%.[5] A more rigorous assessment of heat losses throughout the biorefinery is required to verify the accuracy of a 95% heat transfer efficiency assumption.

Table S2. Unit operation modelling, design, and purchase cost correlations in BioSTEAM.

Unit Operation	BioSTEAM 2.20	Selection	Modeling	Design	Capital Cost Size Factors	References
Pump	Pump	Centrifugal single Centrifugal double Gear Metering plunger	Specify outlet pressure	Based on break and motor efficiency, and NEMA standard motor sizes.	Volumetric flow rate Head Power	Seider (2017) pp. 450-455.[6]
Heat Exchanger (Shell and tube)	HXutility HXprocess	Floating head Fixed head U tube Kettle vaporizer Double pipe	Vapor-liquid equilibrium [Specify temperature or vapor fraction assuming constant pressure]	Heat transfer coefficients based on typical values for selected fluids. Counter current flow.	Heat transfer area	Seider (2017) pp. 316-336, 461-463.[6]
Distillation	ShortcutColumn	-	Fenske-Underwood-Gilliland (FUG)	Based on flooding velocity and tray efficiency.	Vessel weight, inner diameter, and length Number of trays	Seider (2017) pp. 392-395, 464-468.[6] Green (2018) Chapter 13.[7] Duss (2018).[8]
Cooling tower	CoolingTower	-	Specify outlet temperature	-	Volumetric flow rate	Seider (2017) pp. 481-485[6]
Liquids centrifuge	LiquidSplitCentrifuge	General separator	Component splits based on liquid-liquid equilibrium	-	Volumetric flow rate	Apostolakou (2009)[9]

Table S2. Continued…

Unit Operation	BioSTEAM 2.20	Selection	Modeling	Design	Capital Cost Size Factors	References
Tank	MixTank StorageTank	Mix tank Storage tank	-	-	Vessel volume	Apostolakou (2009)[9]
Steam and electricity co-generation system	BoilerTurbogenerator	Complete package	Based on heats of combustions, and boiler and turbogeneration efficiencies.	-	Mass flow rate Power generated	Humbird (2011)[2]

Table S3. Unit operation modelling, design, and purchase cost correlations introduced in this study.

Unit Operation	biorefineries.LAOs	Selection	Modeling	Design	Capital Cost Size Factors	References
Adiabatic Fixed-Bed Dehydration Reactor	AdiabaticFixedbedGasReactor	Pressure vessel	Stoichiometric reaction efficiency	Weight hour space velocity	Vessel weight, Catalyst weight	Seider (2017) pp. 464-466.[6]
Mixer-Settler	MixerSettler	Pressure vessel	Component splits based on liquid-liquid equilibrium	Mixing tank: 5 min residence time 1:1 aspect ratio. Settler: 4:1 aspect ratio 0.1 $ft^2 \cdot$gpm settling area to feed flow	Vessel weight	Seider (2017) pp. 464-472.[6]
Fermentation	Fermentation	Batch agitated	Stoichiometric reaction efficiency	Residence time and reactor volume	Vessel volume, Duty (to cost heat exchangers)	Humbird (2011)[2]

Capital and Operating Costs

All techno-economic calculations and the cash flow analysis were made following the assumptions made by Humbird et. al.[2] for the production of cellulosic ethanol from corn stover. Material prices of feeds come from various sources, including text books and literature.[4, 7-10]

Table S4. Capital expenditures.

	Notes	Lower Scenario Cost [MM$]	Target Scenario Cost [MM$]
ISBL installed equipment cost	-	356	65.6
OSBL installed equipment cost	-	66.5	32.4
Warehouse	4.0% of ISBL	14.2	2.62
Site development	9.0% of ISBL	32.0	5.90
Additional piping	4.5% of ISBL	16.0	2.95
Total direct cost (TDC)	-	484	109
Proratable costs	10.0% of TDC	48.5	10.9
Field expenses	10.0% of TDC	48.5	10.9
Construction	20.0% of TDC	96.9	21.9
Contingency	30.0% of TDC	145	32.8
Other indirect costs (start-up, permits, etc.)	10.0% of TDC	48.5	10.9
Total indirect cost	-	388	87.6
Fixed capital investment (FCI)	-	872	197
Working capital	5.0% of FCI	43.6	9.85
Total capital investment (TCI)	-	916	207

Table S5. Variable operating costs.

		Price [$·ton^{-1}]	Baseline Fermentation Performance Scenario Cost [MM$·yr^{-1}]	Target Fermentation Performance Scenario Cost [MM$·yr^{-1}]	Reference
Raw materials	**Process water**	0.320	9.49	0.995	Seider (2017) pp. 500[6]
	Tridecane	878.15	0.0228	0.00240	*U.S. EIA[11]
	DAP	895	11.2	1.18	Humbird (2011)[2]
	****Glucose**	50, 240, 350	238±39	149±25	Cheng (2018)[3]
	Salt	136	40.2	4.23	The Economist[12]
	CSL	51.5	4.76	0.567	Humbird (2011)[2]
	Natural gas	198	16.4	3.95	Huang (2016)[13]
Waste	**Wastewater treatment [organics]**	-300	-34.2	-6.27	Seider (2017) pp. 500[6]
Total variable operating cost			348±39	162±25	

*Average price from Jan 2015 to Aug 2020.

** Glucose prices correspond to the minimum, most probable, and maximum values of a triangular probability distribution. The material cost of glucose per year is presented as the mean plus or minus one standard deviation.

Table S6. Fixed operating costs.

	Notes	Baseline Fermentation Performance Scenario Cost [MM$·yr^{-1}]	Target Fermentation Performance Scenario Cost [MM$ ·yr^{-1}]
Labor salary	-	2.40	2.40
Labor burden	90% of labor salary	2.25	2.16
Maintenance	3.0% of ISBL	10.7	1.88
Property insurance	3.0% of ISBL	2.50	0.441

Table S7. Economic metrics.

	Baseline Fermentation Performance Scenario	Target Fermentation Performance Scenario
MPSP [$·ton^{-1}]	3350±275	1390±172

Accessing Biorefinery Models and Detailed Results

All biorefinery source code and excel results are available in the BioSTEAM Bioindustrial-Park GitHub repository,[6] a standard repository for complete biorefinery models and results to foster accessibility and deeper communication within the biorefinery simulation community. The specific BioSTEAM version used to generate the results is noted for each set of results as future BioSTEAM versions may include more rigorous thermodynamic models and/or assumptions that may alter results. The repository also includes flowsheets, utility requirements, design requirements, itemized costs, cash flow analysis for each biorefinery. A tutorial on how to use the biorefinery models is detailed in the BioSTEAM documentation.[3]

FAME analysis of the Tridecane Sample

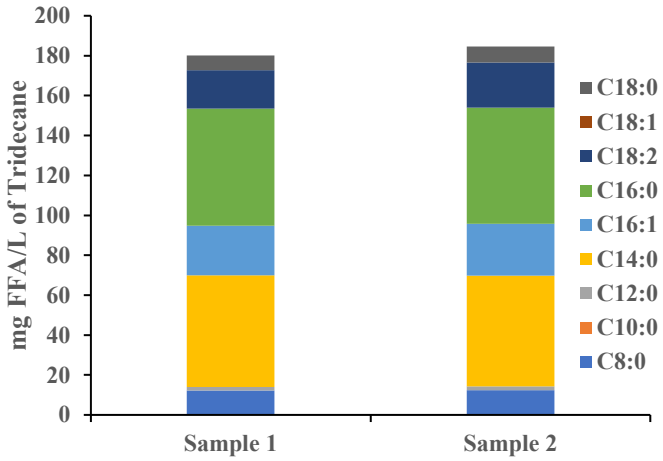

Figure S3. Two 2.5 mL samples of the biologically derived tridecane fatty alcohol feed were analyzed with FAME analysis and ran on GC-FID as previously described.[14] These two samples describe the concentration of FFA observed in the feed which are likely derived from lipids or intermediate FFA species in the sample. Note that FAME analysis requires complete drying of the samples for conversion of lipid and FFA species to their respective FAMEs. After FAME analysis, samples are resuspended in hexane for GC-FID analysis. Due to the high boiling point of tridecane, these samples could not be fully evaporated via speed vac and lyophilization for FAME analysis. Although the samples had any water removed, the remaining tridecane likely lead to an underestimate of the final concentration of the FAME samples when resuspended in hexane analyzed by GC-FID. Additionally, the values for C10-C14 FFA are likely skewed due the large remaining tridecane peak observed. For this reason and for simplicity only C_8 and C_{16} FFA species were considered for poisoning studies.

References

1. A. Z. Elvira Greiner; Bland, E.; Kumamoto, T., *Linear Alpha-Olefins Chemical Economics Handbook.*, IHS Markit, 2020.
2. D. D. Humbird, R.; Tao, L.; Kinchin, C.; Hsu, D.; Aden, A.; Schoen, P.; Lukas, J.; Olthof, B.; Worley, M.; Sexton, D.; Dudgeon, D., *Process Design and Economics for Biochemical Conversion of Lignocellulosic Biomass to Ethanol: Dilute-Acid Pretreatment and Enzymatic Hydrolysis of Corn Stover;*, DOE: NREL, 2011.
3. M. H. Cheng, H.; Dien, B. S.; Singh, V., *Biofuels Bioprod. Biorefining*, 2019, **13**, 723-739.

4. Y. K. Cortes-Peña, D.; Singh, V.; Guest, J. S., *ACS Sustain. Chem. Eng.*, 2020, **8**, 3302-3310.
5. Y. R. Cortes-Pena, 2019.
6. W. D. L. Seider, D. R.; Seader, J. D.; Widagdo, S.; Gani, R.; Ng, M. K, in *Product and Process Design Principles*, Wiley, 2017, pp. 426-485.
7. D. W. Green, *Perry's Chemical Engineers' Handbook 9th Edition*, McGraw-Hill Education, New York, NY, 2018.
8. M. T. Duss, R., 2018.
9. A. A. K. Apostolakou, I. K.; Marazioti, C.; Angelopoulos, K. C., *Fuel Process. Technol.*, 2009, **90**, 1023-1031.
10. Y. R. G. Cortes-Pena, J. S., 2019.
11. U.S. On-Highway Diesel Fuel Prices, (accessed September 11, 2020).
12. *Journal*, 2010.
13. H. L. Huang, S.; Singh, V., *Biofuels Bioprod. Biorefining*, 2016, **10**, 299-315.
14. N. J. Hernández Lozada, R.-Y. Lai, T. R. Simmons, K. A. Thomas, R. Chowdhury, C. D. Maranas and B. F. Pfleger, *ACS Synthetic Biology*, 2018, **7**, 2205-2215.